A Study on Mitigation Strategies for Thermal Loads on Piping Systems Induced by Thermal Stratification in Nuclear Power Plants

Sung-in Jung, Youn-ho Cho*

Department of Nuclear Engineering, Pusan National University, Busan, Republic of Korea
**Corresponding author: mechcyh@pusan.ac.kr*

Abstract

Thermal stratification occurring in piping systems of operating nuclear power plants induces significant circumferential temperature differences, leading to bending stresses and cumulative thermal fatigue damage. In Korea, verification of piping integrity against thermal stratification has become a mandatory requirement during long-term operation license renewal reviews. However, most previous studies have focused on evaluating thermal stratification or fatigue damage, while practical mitigation techniques applicable to operating plants remain limited. This study proposes a passive thermal mitigation device, referred to as a Passive Thermal Reliever (PTR), which is externally attached to the pipe surface to enhance circumferential heat conduction. Three-dimensional transient heat transfer analyses were conducted to quantitatively evaluate the mitigation performance of the proposed PTR device. The results demonstrate that the PTR effectively reduces upper–lower temperature differences without modifying the internal pipe structure, indicating its applicability as a practical solution for mitigating thermal stratification–induced thermal loads in operating nuclear power plants.

***Keywords :** Thermal stratification; Thermal load; Mitigation; Passive thermal reliever; Heat transfer;*

1. Introduction

Thermal stratification is a well-known phenomenon in piping systems of pressurized water reactors, particularly in stagnant or low-flow branch lines. Under such conditions, hot and cold coolant layers may separate within the pipe, resulting in asymmetric circumferential temperature distributions. These temperature gradients induce bending stresses in the pipe wall and accelerate thermal fatigue damage through repeated thermal cycling. As an increasing number of nuclear power plants approach or exceed their original design lifetimes, long-term operation license renewal has become a critical issue. Accordingly, regulatory authorities require comprehensive re-evaluation of piping integrity, including the effects of thermal stratification. Despite extensive studies on stratification assessment, practical mitigation measures applicable to operating plants remain insufficient.

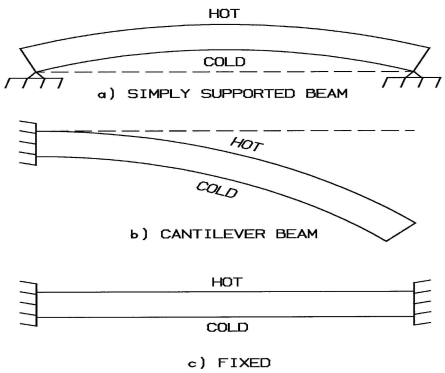

Fig 1. Bending stress induced by thermal stratification (Source: EPRI TR-103581)

2. Regulatory Background and Previous Studies

Regulatory guidance on thermal stratification has been established through a series of bulletins and technical reports, including USNRC Bulletins 88-08 and 88-11 and EPRI guidelines such as MRP-146. These documents provide criteria for identifying susceptible piping locations and evaluating thermal fatigue damage. Numerous analytical and experimental studies have been conducted to characterize stratification behavior, temperature distributions, and fatigue implications. Computational fluid dynamics analyses have been widely used to simulate stratified flow fields, while field measurements have provided valuable validation data. Despite this extensive body of research, most efforts have focused on assessment rather than mitigation.

3. Limitations of Existing Mitigation Approaches

Korean domestic research on thermal stratification can be broadly classified into two main categories:

a. analytical evaluations of thermal stratified flow of internal fluids and temperature gradients within the fluid and,

b. assessments of bending stress and fatigue resulting from temperature differences between the upper and lower regions of the fluid inside piping.

These studies have been utilized in the design of new nuclear power plants to prevent the occurrence of thermal stratification by reflecting evaluation results at the design stage. However, for piping in aging domestic nuclear power plants where thermal stratification is already occurring, current practices are largely limited to

fatigue evaluation followed by periodic nondestructive inspection. Research in Korea on mitigation measures for thermal fatigue in piping with pre-existing thermal stratification remains insufficient.

In this regard, some previous studies and patents have proposed mitigating thermal stratification by applying heat tracing to the lower portion of the pressurizer surge line, or by installing anti-stratification structures inside the surge line to prevent the formation of stratified flow. However, due to limitations in the field applicability of these prior approaches, they have not been applied to operating nuclear power plants in Korea.

Several mitigation concepts have been proposed to reduce thermal stratification effects, including heat tracing of surge lines and installation of internal flow-mixing devices. Heat tracing can reduce temperature gradients but may increase overall pipe temperature and thermal expansion, leading to higher loads on pipe supports and restraints. Internal mixing devices can promote fluid mixing but introduce concerns related to flow obstruction, mechanical wear, and inspection challenges. As a result, these approaches have not been widely adopted in operating nuclear power plants, highlighting the need for alternative mitigation strategies for operating nuclear power plants in korea.

4. Concept of Passive Thermal Reliever

In this study, a Passive Thermal Reliever (hereafter PTR) device is proposed as a practical mitigation method. The PTR is externally attached to the pipe surface and designed to promote circumferential heat conduction from the hot upper region to the cooler lower region. By utilizing material thermal conductivity, the PTR passively redistributes heat without requiring additional power or control systems. Because the PTR does not alter the internal geometry, it can be readily applied to existing piping systems.

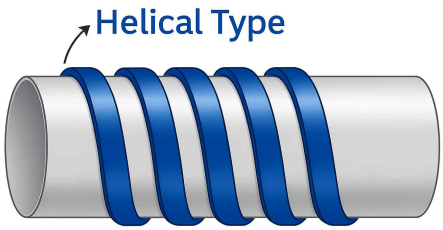

Fig 2. Concept of PTR Device

5. One-Dimensional Circumferential Thermal Analysis for PTR Material Selection

For the PTR device material, two candidates—an aluminum alloy and a copper alloy (with a Cu content of 99.95% or higher)—were selected to evaluate their thermal mitigation performance. These materials exhibit thermal conductivities significantly higher than that of the existing austenitic stainless steel piping (hereafter referred to as 316SS) and are commonly used in industrial applications, while also accounting for installation loads and structural considerations.

The reasons for selecting these two materials are as follows.

a. Heat transfer perspective:
Copper alloys with purity close to that of pure copper exhibit slightly lower thermal conductivity than silver; however, among metallic materials commonly used in industrial applications, they can be regarded as having the highest thermal conductivity. In particular, their thermal conductivity is at least 20 times greater than that of 316SS. Nevertheless, due to their relatively high density, geometric constraints may arise when weight allowance is considered.

b. Structural load perspective:
Aluminum alloys have a lower thermal conductivity than copper alloys but still exhibit approximately ten times higher thermal conductivity than 316SS. Moreover, their density is approximately one-third that of 316SS, making them advantageous in terms of additional installation loads (dead weight) when applied to piping systems.

To comparatively evaluate the heat conduction capability of the selected PTR materials and the existing piping, the one-dimensional circumferential heat transfer governing equation was applied as follows.

The governing equation for heat conduction in a pipe expressed in a cylindrical coordinate system (r, θ, z) is given as:

$$\frac{1}{r}\frac{\partial}{\partial r}(kr\frac{\partial T}{\partial r}) + \frac{1}{r^2}\frac{\partial}{\partial \theta}(k\frac{\partial T}{\partial \theta}) + \frac{\partial}{\partial z}(k\frac{\partial T}{\partial z}) + \dot{q} = \rho c_p \frac{\partial T}{\partial t}$$

where
q̇ : volumetric heat generation rate
k : thermal conductivity
ρ : material density
c_p : specific heat capacity
T : temperature as a function of r, θ, and z
t : time

Assuming the thermal conductivity k is constant, the governing equation can be rewritten as:

$$k\nabla^2 T + \dot{q} = \rho c_p \frac{\partial T}{\partial t}$$

To evaluate the one-dimensional circumferential (θ) heat transfer capability of the existing piping and material-specific PTR devices, the radial (r) and axial (z) temperature gradients are neglected, and the volumetric heat generation rate is assumed to be zero. Under these assumptions, the governing equation reduces to:

$$\frac{\partial T}{\partial t} = \alpha \frac{1}{r^2}\frac{\partial^2 T}{\partial \theta^2}, \quad \alpha = \frac{k}{\rho c_p}$$

where α is the thermal diffusivity, and the domain is defined as $0 \le \theta < 2\pi$ and $t > 0$.

The initial and boundary conditions are defined as follows:

Initial condition: T(θ, 0) = f(θ), an arbitrary 2π-periodic function, assuming no external heating/cooling or θ-dependent convection.

Boundary condition (periodicity): T(0, t) = T(2π, t), ∂T/∂θ |_{θ=0} = ∂T/∂θ |_{θ=2π}

$$T_{avg} = \frac{1}{2\pi}\int_0^{2\pi} f(\theta)d\theta$$

$$\frac{d}{dt}\left(\frac{1}{2\pi}\int_0^{2\pi} T d\theta\right) = \frac{\alpha}{2\pi r^2}\int_0^{2\pi}\frac{\partial^2 T}{\partial\theta^2}d\theta = \frac{\alpha}{2\pi r^2}\frac{\partial T}{\partial\theta}\Big|_0^{2\pi} = 0\,(Periodicity)$$

$$\therefore \frac{dT_{avg}}{dt} = 0$$

The circumferential temperature can be expressed as the sum of the average temperature T_avg and a temperature fluctuation function u(θ, t):

$$T(\theta,t) = T_{avg} + u(\theta,t)$$

The governing equation for the temperature fluctuation function becomes:

$$\frac{\partial u}{\partial t} = \alpha\frac{1}{r^2}\frac{\partial^2 u}{\partial\theta^2}$$

$$u(0,t) = u(2\pi,t),\ \frac{\partial u}{\partial\theta}(0,t) = \frac{\partial u}{\partial\theta}(2\pi,t),\ u(\theta,0) = f(\theta) - T_{avg}$$

Assuming a separable solution u(θ, t) = X(θ) Y(t), the equation can be separated into two ordinary differential equations with a separation constant λ:

$$X(\theta)\,Y'(t) = \alpha\frac{1}{r^2}X''(\theta)\,Y(t)$$

$$\Rightarrow \frac{Y'}{\alpha Y/r^2} = \frac{X''}{X} = -\lambda,\quad \lambda = n^2\,(n = order)$$

By solving these equations, the general solution for the temperature fluctuation function is obtained as:

$$u(\theta,t) = \sum_{n=1}^{\infty}\left[A_n\cos(n\theta) + B_n\sin(n\theta)\right]e^{-(\alpha n^2/r^2)t}$$

$$A_n = \frac{1}{\pi}\int_0^{2\pi} u(\theta,0)\cos(n\theta)d\theta,\quad B_n = \frac{1}{\pi}\int_0^{2\pi} u(\theta,0)\sin(n\theta)d\theta$$

For n = 0, the eigenvalue λ = 0, which represents the average temperature mode. Temperature fluctuations occur for n ≥ 1. Since the decay rate α n² / r² increases with the mode number, higher-order modes decay more rapidly.

Thermal stratification in piping exhibits upper–lower thermal asymmetry, which can be regarded as a left–right symmetric initial condition in the circumferential direction. According to the orthogonality condition for even symmetry, the sine coefficients vanish, i.e., Bn = 0.

$$\therefore T(\theta,t) = T_{avg} + \sum_{n=1}^{\infty} A_n\cos(n\theta)\,e^{-(\alpha n^2/r^2)t}$$

$$A_n = \frac{1}{\pi}\int_0^{2\pi} u(\theta,0)\cos(n\theta)d\theta = \frac{2\triangle}{\pi}\frac{\sin(\frac{n\pi}{2})}{n},\ \triangle = T_{top} - T_{bottom}$$

$$A_{2k} = 0,\ A_{2k-1} = (-1)^{k-1}\frac{2\triangle}{(2k-1)\pi}$$

According to the heat conduction governing equation, the one-dimensional circumferential thermal diffusion capability of each material is as follows.

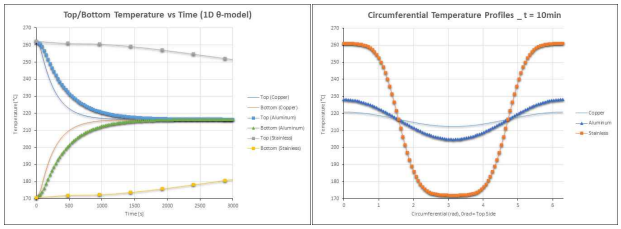

Fig 3. Comparison of Thermal Diffusion Capability by Material

Table 1. Time Required for Upper–Lower Pipe Temperature Equalization (< 0.3 °C)

Material	Required Time
Austenitic Stainless Steel (SA-312 TP316)	Approximately 632 min
Aluminum Alloy (SB-209 A96061 T651)	Approximately 38 min
Copper Alloy (SB-152 C10200 H00)	Approximately 23 min

6. Thermal Analysis Methodology

Three-dimensional transient heat transfer analyses were performed using a finite element approach. Two baseline numerical configurations were considered: a three-layer model consisting of fluid, pipe, and insulation, and a five-layer model including thermal grease and a Passive Thermal Reliever (PTR) device.

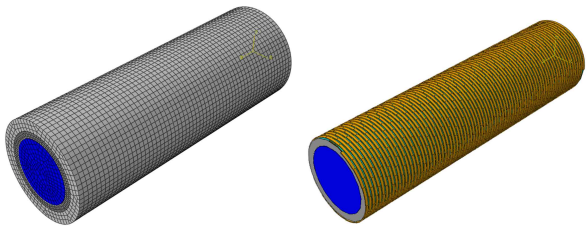

Fig 4. (Left) 3-Layer Model, (Right) 5-Layer Model

For the PTR device, the geometrically most favorable configuration for heat transfer would be a fully cylindrical (sleeve-type) geometry that allows complete contact with the pipe surface. However, such a configuration cannot be installed without cutting the existing piping and may induce additional thermal stresses in the pipe due to differences in thermal expansion between dissimilar materials. Therefore, to ensure practical applicability in actual plant conditions, a helical-type geometry, as shown in Fig 2, is proposed for the PTR device.

The allowable load of the PTR device is constrained to remain within ±10% of the pipe weight, corresponding to a maximum of 20 kgf/m. Since the PTR device installed on the pipe distributes its load uniformly along the pipe, it can be treated as a uniformly distributed weight. Therefore, in accordance with the EPRI NP-5639, Guidelines for Piping System Reconciliation (NCIG-05,

Revision 1), which specifies an allowable weight variation of ±20% of the piping analysis weight, the PTR device geometry is conservatively designed such that its additional weight does not exceed 10% of the existing pipe weight (20 kgf/m).

Accordingly, the PTR device geometry must be designed to satisfy this load limitation. Based on the geometric parameters of the PTR device, the maximum allowable thickness for each material is presented in table 2.

Based on combinations of model configuration, PTR material, and geometric parameters, a total of six numerical models were constructed and analyzed in this study. Initial and boundary conditions were defined based on measured plant operating data and conservative assumptions for ambient heat transfer through insulation. Radiative heat transfer effects were neglected due to their relatively minor contribution under the considered conditions.

Table 2. Geometry of the PTR Device for Different Materials

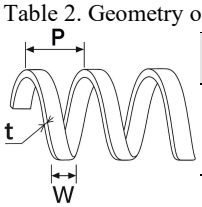

Material	Model	W [mm]	P [mm]	t_{max} [mm]
Copper Alloy	Model-1	10	15	3.0
	Model-2	10	30	6.0
	Model-3	25	30	2.5
Aluminum Alloy	Model-4	10	15	10
	Model-5	25	30	9.0
	Model-6	10	15	3.0

The initial conditions (t=0) for the finite element analysis were based on measured data obtained from the actual plant.

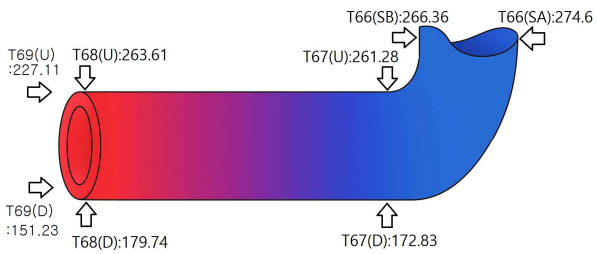

Fig 5. Initial thermal condition at the pipe outer wall [°C]

For the heat transfer analysis, the analytical model shown in Fig 4 was adopted, consisting of a fluid ↔ pipe ↔ thermal grease ↔ PTR device ↔ insulation ↔ ambient air configuration. For each layer, a perfect thermal contact condition was imposed, ensuring continuity of the temperature field across all interfaces. The mesh was composed of three-dimensional diffusion continuum elements (DC3D8, Diffusion Continuum 3D Hexahedral)[37], which are suitable for heat transfer analysis.

The temperature field at the inner wall of the pipe, $T(\theta,z)$, was assumed to vary linearly using the measured values. This assumption of a linear temperature distribution is considered conservative for heat transfer analysis.

Here, the temperature boundary conditions are defined as follows:

$$f = \frac{1}{2} - \frac{Y}{2R_i},\ T(\theta, z) = (1 - f)\, T_{top}(z) + f\, T_{bottom}$$

Where,

Upper side (+Y): T=$T68(U)$ at z=0 and T=$T67(U)$ at z=L

Lower side (−Y): T=$T68(D)$ at z=0 and T=$T67(D)$ at t z=L

Ri denotes the inner radius of the pipe.

Since the primary focus of the thermal analysis is the heat mitigation effect of the PTR device, the pipe end locations corresponding to measurement points T69 (downstream of the check valve) and T66 were treated as adiabatic boundaries, reflecting the actual high-temperature operating conditions.

7. Results and Discussion

a. 3-Layer Model

Before evaluate the heat mitigation effect of the PTR device, a transient heat transfer analysis was performed on a simplified three-layer structure consisting of fluid–pipe–insulation, applying the same initial and boundary conditions as those used in the PTR device model.

Since the structural configuration is relatively simple and the analysis focuses primarily on heat transfer behavior, the total number of nodes was limited to fewer than 100,000 in order to reduce computational time.

Table 3. Mesh Information of 3-Layer Model

Component	Element	Total Node
Fluid	12,322	74,524
Pipe	34,038	
Insulation	10,980	

In the absence of internal heat generation, the time required for the upper and lower temperatures at the inner wall of the pipe to reach thermal equilibrium (temperature difference < 0.3 °C) was found to be approximately 19 hours (68,400s). To verify the reliability of the analysis results, an additional simulation was conducted under the condition of no internal fluid, in which the time required for the upper and lower temperatures to reach equilibrium was approximately 560 minutes. This result is in good agreement with the one-dimensional circumferential heat transfer calculation presented in table 1, which yielded a value of approximately 632 minutes, confirming that the applied initial and boundary conditions are appropriate.

The slightly shorter equilibration time obtained from the present analysis compared to the one-dimensional circumferential(θ) heat transfer calculation can be attributed to the three-dimensional nature of the model,

in which heat is dissipated not only in the circumferential direction but also in the radial (r) and axial (z) directions. As a result, thermal equilibrium is achieved more rapidly than in the simplified one-dimensional circumferential heat transfer model.

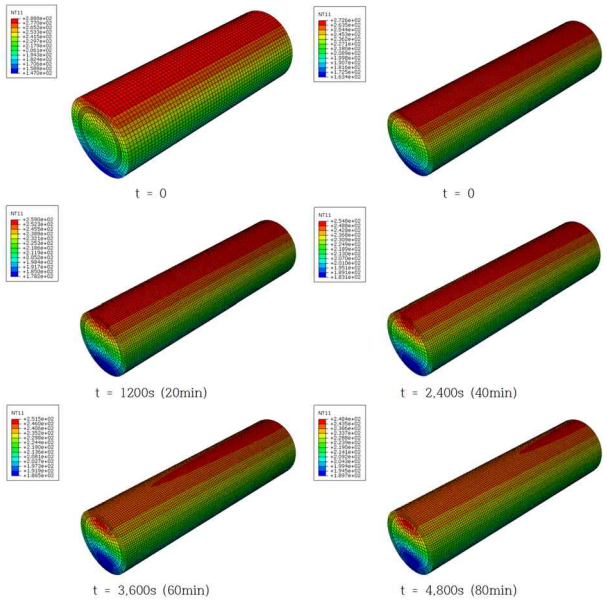

Fig 6. Heat transfer analysis results of the 3-layer model

b. 5-Layer Model

The baseline three-layer model exhibited a slow reduction in circumferential temperature difference, indicating persistent thermal stratification. In contrast, the PTR-installed model showed a significantly faster reduction in upper–lower temperature difference. Aluminum alloy PTR devices provided a favorable balance between thermal performance and additional dead weight, whereas copper alloy PTR devices showed faster response but higher weight penalties.

When the PTR device is installed, the upper–lower temperature difference (ΔT) of the pipe decreases significantly within a short period of time and rapidly converges to below the conservative threshold value, ΔT < 50°F, specified in EPRI MRP-146 for assessing the integrity of thermally stratified piping.

Table 4. Mesh Information of 5-Layer Model

Component	Element						Total Node					
	Model-1	Model-2	Model-3	Model-4	Model-5	Model-6	Model-1	Model-2	Model-3	Model-4	Model-5	Model-6
Fluid	12,322	12,322	12,322	12,322	12,322	12,322	109,078	83,338	173,448	116,600	92,026	109,078
Pipe	12,393	12,393	12,393	12,393	12,393	12,393						
Thermal Grease	5,508	5,508	5,508	5,508	5,508	5,508						
PTR Device	16,394	8,204	49,154	18,736	12,299	16,394						
Insulation	10,980	10,980	10,980	10,980	10,980	10,980						

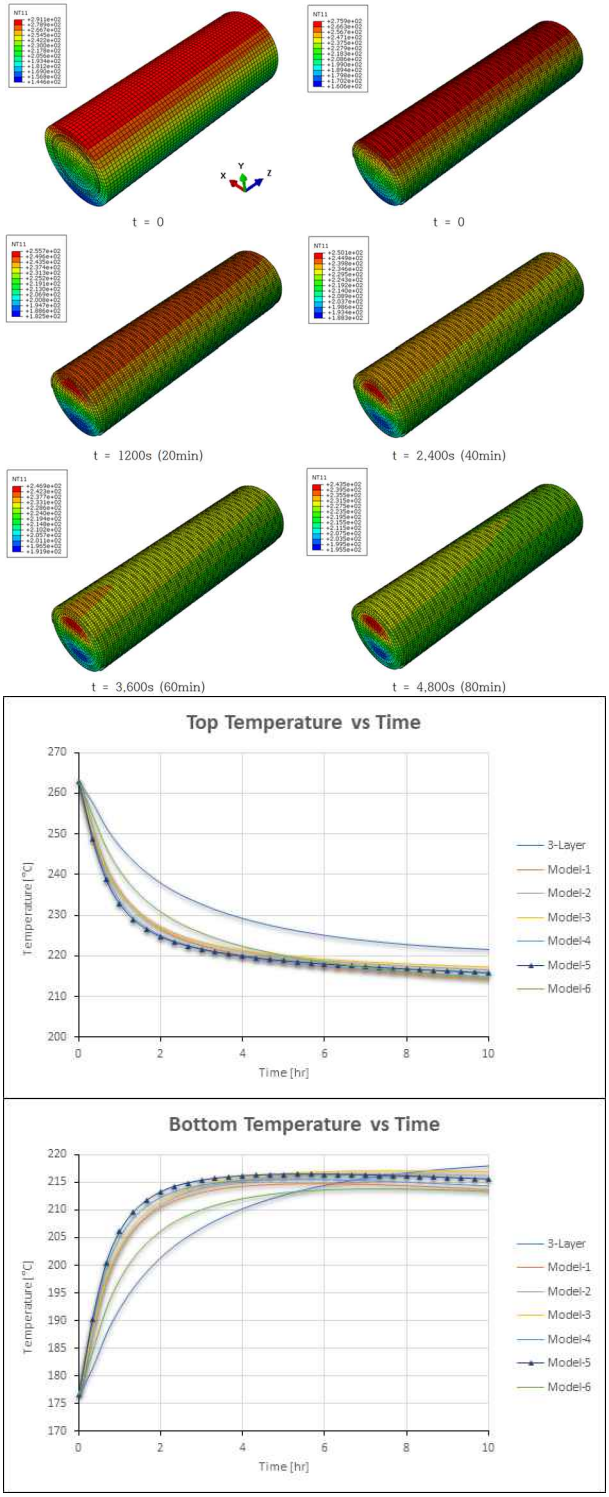

Fig 7. Time-dependent temperature variations at the upper and lower inner wall of the pipe for each model

In particular, the Model-5 demonstrated that ΔT converged to below the threshold within approximately one hour.

Due to the PTR device, heat from the pipe outer surface is rapidly dissipated in both the circumferential and axial directions, resulting in a larger amount of heat loss through the insulation compared to the three-layer model. Consequently, the equilibrium temperatures of the upper and lower regions of the pipe gradually decrease with time. This effect reduces the overall thermal expansion of the pipe, thereby mitigating the risk of excessive thermal deformation–induced damage. In addition, the reduced thermal expansion provides additional margin for allowable loads on pipe supports, indicating a positive impact on overall piping integrity.

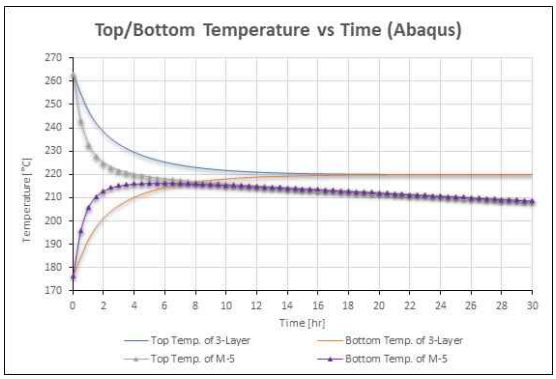

Fig 8. Time-dependent upper and lower pipe wall temperature

For PTR devices with identical geometries (Model-1 vs. Model-6), the copper-alloy PTR device was confirmed to reduce the upper–lower temperature difference (ΔT) more rapidly than the aluminum-alloy PTR device.

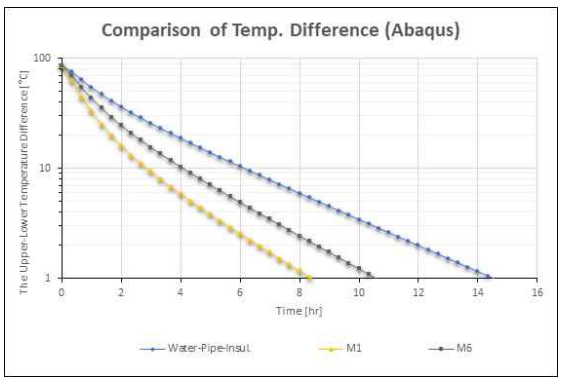

Fig 9. Comparison of time-dependent upper–lower inner wall temperature differences (ΔT) between Model-1 and Model-6

When the PTR geometry was constrained such that the additional weight did not exceed 10% of the pipe weight, the aluminum-alloy PTR device (Model-5) exhibited the greatest thermal mitigation performance. Under identical width and pitch conditions (Model-3 vs. Model-5), the lower density of the aluminum alloy allowed the PTR thickness to be more than three times greater than that of the copper alloy. As a result, the effective radial heat-transfer path through the high-conductivity PTR device was extended, leading to enhanced thermal diffusion performance.

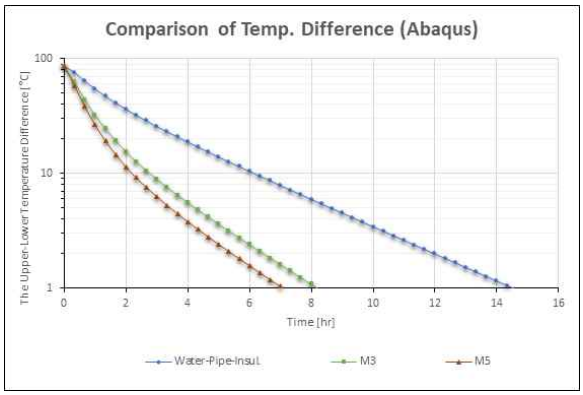

Fig 10. Comparison of time-dependent upper–lower inner wall temperature differences between Model-3 and Model-5

8. Field Applicability

In this study, a sensitivity analysis was conducted to quantitatively evaluate the effects of the presence of internal fluid in the pipe and variations in the thermal properties of the heat transfer medium (thermal grease) between the pipe and the PTR device on the overall thermal response.

a. Fluid Sensitivity

First, cases with and without internal fluid were compared to examine how changes in the thermal capacity of stagnant fluid affect the time required to reach thermal equilibrium and the formation of temperature gradients. As shown in Table 5 and Figure 11, the presence of internal fluid was found to delay the temperature mitigation of the pipe. This behavior can be attributed to the relatively larger heat capacity of the fluid compared to that of the pipe material.

Table 5. Time required to reach upper–lower pipe temperature equilibrium (< 0.3 °C) with and without internal fluid

Description	Required Time
Water-Pipe-Insulation, 3-Layer	Approx. 1,140min
Pipe-Insulation, 2-Layer	Approx. 560min
Water-Pipe-Thermal Grease-PTR Device-Insulation, 5-Layer (Model-1)	Approx. 680min
Pipe-Thermal Grease-PTR Device-Insulation, 4-Layer (Model-1)	Approx. 240min

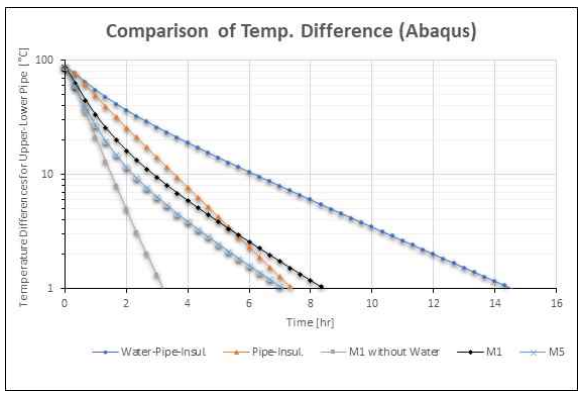

Fig 11. Time-dependent upper–lower inner wall temperature difference (ΔT) of the pipe with and without internal fluid

When the PTR device is installed, as illustrated in Figure 11, the temperature difference between the upper and lower inner wall of the pipe (ΔT) decreases more rapidly than in the pipe–insulation two-layer model without internal fluid. However, as the temperature difference becomes smaller, the time required to reach thermal equilibrium increases. This indicates that the effectiveness of the PTR device is more pronounced when the temperature difference between the upper and lower regions is large. In addition, for a specific configuration (Model-5), thermal equilibrium was achieved faster than in the two-layer model.

b. Thermal Grease Sensitivity

A sensitivity analysis was also performed by varying the thermal properties of the thermal grease—particularly thermal conductivity and specific heat—to investigate the influence of changes in thermal contact resistance on both local and global heat transfer mechanisms. In practical applications, conservative conditions were considered to account for potential degradation scenarios, such as thermal grease flowing downward along the pipe due to gravity or insufficient application resulting from installation errors.

CASE-1: The thermal grease layer (0.015 mm) is assumed to have completely evaporated and been replaced by an air layer.

CASE-2: A 1 mm thick cylindrical air gap is assumed to exist between the pipe and the PTR device, representing a condition in which heat transfer occurs through an air layer without direct contact.

For CASE-1 and CASE-2, the cylindrical air gap was conservatively modeled as having a uniform circumferential clearance along the pipe. The PTR device configuration selected for this analysis was Model-5, which provides the most effective heat mitigation performance.

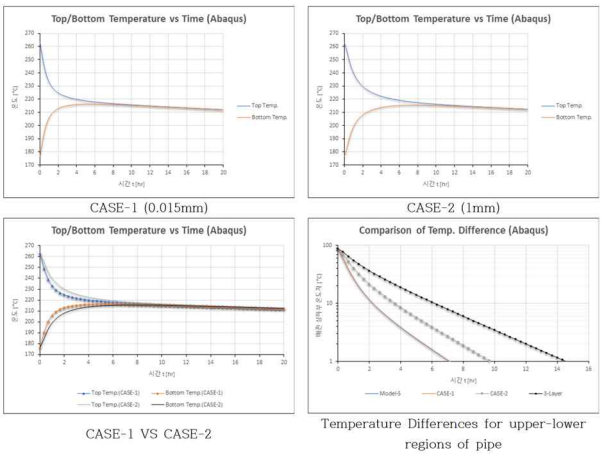

Fig 12. Time-dependent variations of upper and lower pipe inner wall temperatures for each case

The results of the thermal grease sensitivity analysis indicate that, in CASE-1, the temperature difference between the upper and lower inner wall of the pipe (ΔT) is generally about 0.1–0.4 °C higher than that of the thermal grease case over the 0–4 hour time range, suggesting that the impact is relatively minor. In contrast, although CASE-2 still demonstrates a clear improvement compared to the three-layer model without a PTR device, the low thermal properties of the air layer delay the mitigation of the upper–lower temperature difference.

Table 6. Comparison of upper–lower temperature difference (ΔT) variations by case over 0–120 minutes

Description	Upper-Lower Temperature Difference (ΔT) Variations [°C]	Ratio (Description vs Model-5)
Model-5	74.82	100% (-)
CASE-1	74.60	99.7% (-0.3% ↓)
CASE-2	64.76	86.6% (-13.4% ↓)
3-Layer	49.93	66.7% (-33.3% ↓)

As summarized in Table 6, even if partial debonding or insufficient application of thermal grease occurs during installation of the PTR device, the resulting reduction in heat mitigation performance is expected to be within approximately 13.4% (CASE-2) relative to the ideal PTR device performance.

9. Conclusions

Considering Korean domestic power supply and demand issues and the changing energy environment—such as the transition to the AI era and carbon neutrality—it is not feasible to meet the continuously increasing electricity demand solely through the unlimited construction of new nuclear power plants. Therefore, continued operation of aging nuclear power plants whose initial operating license periods have expired is an essential consideration. For the continued operation of aging plants, the integrity of a wide range of components must be ensured so that safe and stable operation can be maintained throughout the extended licensing period.

In this study, a PTR device capable of mitigating thermal stratification formed in Safety Class 1 piping of operating nuclear power plants was developed, and a geometry applicable to actual plant conditions was proposed. In addition, the thermal mitigation performance of the PTR device was evaluated for different materials and geometrical configurations.

At present, there are no mitigation measures actively applied to operating nuclear power plants that can alleviate thermal stratification without modifying the piping geometry through design changes. The Passive Thermal Reliever (PTR) proposed in this study can be easily installed without altering the existing piping geometry, making it highly applicable to field conditions. When applied in practice, the PTR device is expected to rapidly reduce the upper–lower temperature difference (ΔT) of thermally stratified piping in aging nuclear power plants, thereby mitigating thermally induced loads

caused by stratification and ensuring sufficient piping integrity during the continued operation period.

The main conclusions regarding the effectiveness of the PTR device derived from this study are summarized as follows.

a. Heat Mitigation Effect of the PTR Device

When the PTR device is installed, the temperature difference between the upper and lower regions of the pipe (ΔT) decreases significantly within a short time. It was confirmed that ΔT rapidly converges below the conservative threshold value, $\Delta T_{threshold}$ = 50 °F, specified in EPRI MRP-146 as a criterion for evaluating the integrity of thermally stratified piping. For Model-5, this convergence occurred within one hour.

The PTR device promotes rapid dissipation of heat from the outer surface of the pipe in both the circumferential and axial directions, allowing more heat to be released through the insulation compared to the three-layer model without the PTR device. As a result, the equilibrium temperatures of the upper and lower regions of the pipe gradually decrease over time. This effect reduces thermal expansion of the pipe, preventing damage caused by excessive thermal deformation, and provides additional margin with respect to allowable loads on pipe supports, thereby positively contributing to piping integrity.

For identical geometries (Model-1 vs. Model-6), the copper alloy PTR device was found to reduce the upper–lower temperature difference (ΔT) more rapidly than the aluminum alloy PTR device as illustrated in Figure 9.

When the PTR device geometry is constrained such that its weight does not exceed 10% of the pipe weight, the model exhibiting the greatest heat mitigation performance was identified as the aluminum alloy PTR device (Model-5). For the same width and pitch (Model-3 vs. Model-5), the lower density of the aluminum alloy allows the thickness to be increased by more than three times compared to the copper alloy. As a result, the radial heat transfer path through the high-thermal-conductivity PTR device becomes longer, enhancing heat diffusion performance as illustrated in Figure 10.

b. Evaluation of Field Applicability

To evaluate field applicability, the sensitivity analyses described in Section 8 were performed. The conclusions regarding field applicability based on the sensitivity analysis results are as follows.

As pipe diameter increases, the volume of internal fluid increases, resulting in a relatively larger thermal capacity of the fluid compared to that of the pipe. Based on the fluid sensitivity analysis, the heat mitigation effect of the PTR device is expected to be more pronounced for smaller-diameter pipes.

During field installation of the PTR device, gaps may exist between the pipe and the PTR device due to construction quality or installation errors. According to the thermal grease sensitivity analysis, even under conservative conditions where a 1 mm air gap exists, sufficient heat mitigation performance can still be expected when the PTR device is installed.

The geometric constraint of the PTR device was conservatively limited to 10% of the pipe weight. However, in actual field applications, the PTR device geometry can be selected based on the maximum allowable additional load determined through review of piping stress analysis reports. If the allowable additional load exceeds the 10% pipe weight assumed in this study, the heat mitigation performance of the PTR device is expected to further improve.

c. Consideration of Local Thermal Stress Effects

The installation of the PTR device was confirmed to mitigate thermal loads by reducing the circumferential temperature difference between the upper and lower regions of the pipe, thereby contributing to a reduction in global bending stress induced by thermal stratification.

However, due to the structural characteristics of the helical-type PTR, partial non-contact regions inevitably exist between the PTR and the pipe surface. As shown in Table 2, the gap (λ = P − W) is maintained relatively small compared to the contact width (W), such that the influence of localized thermal stresses is minimized by design.

Nevertheless, the potential effects of non-uniform local thermal stresses that may arise in these non-contact regions on the structural integrity and fatigue life of the piping system require further quantitative evaluation through detailed thermo-mechanical coupled analysis.

REFERENCES

[1] U.S. Nuclear Regulatory Commission (USNRC), Bulletin 88-08, Supplement 3: Thermal Stress in Piping Connected to Reactor Coolant System, Washington, DC, 1988.

[2] U.S. Nuclear Regulatory Commission (USNRC), Bulletin 88-11: Pressurizer Surge Line Thermal Stratification, Washington, DC, 1988.

[3] Electric Power Research Institute (EPRI), Thermal Stratification, Cycling, and Striping (TASCS), EPRI TR-103581, Palo Alto, CA, 1994.

[4] Electric Power Research Institute (EPRI), Materials Reliability Program: Management of Thermal Fatigue in Normally Stagnant Non-Isolable Reactor Coolant System Branch Lines, EPRI MRP-146, Revision 2, Palo Alto, CA, 2016.

[5] ASME, Boiler and Pressure Vessel Code, Section III: Rules for Construction of Nuclear Facility Components, American Society of Mechanical Engineers, New York, NY.

[6] ASME, Boiler and Pressure Vessel Code, Section II: Materials, American Society of Mechanical Engineers, New York, NY.

[7] Electric Power Research Institute (EPRI), Guidelines for Piping System Reconciliation, EPRI NP-5639 (NCIG-05, Revision 1), Palo Alto, CA, 1988.
[8] Incropera, F.P., DeWitt, D.P., Bergman, T.L., Lavine, A.S., Fundamentals of Heat and Mass Transfer, 8th ed., John Wiley & Sons, Hoboken, NJ, 2007.
[9] National Bureau of Standards (NBS), National Standard Reference Data Series – National Bureau of Standards 8: Thermodynamic and Transport Properties, Category 5, U.S. Department of Commerce, Washington, DC, 1966.
[10] National Institute of Standards and Technology (NIST), Properties of Copper and Copper Alloys at Cryogenic Temperatures, NIST Monograph 177, Gaithersburg, MD, 1992.